Section 4

Laboratory Measurements and Predictions

The basic equipment for HETG laboratory testing, a Laser Reflection setup and the X-Ray Grating Evaluation Facility (X-GEF), are described in Dewey *et al.*[17] with more details of the X-GEF facility and its operation for flight testing presented in Flanagan *et al.*[24].

The gratings were mounted to the HESS at the HETG Alignment Facility where the average facet roll angle was set and measured based on the polarization alignment technique of Anderson *et al.*[4].

We have used these "sub-assembly" data (along with similar predictions for the HRMA and ACIS-S) to produce predicted curves as a baseline for comparison with the XRCF measurement results and an initial flight prediction.

Table 4.1: HETG laboratory setups and the parameters measured

Parameter	Lab Setup
Period	LR
Period variation	LR
Roll	Alignment
Roll variation	LR
Efficiency	X-GEF

4.1 LR Measurements

4.1.1 LR Period and Roll Variations

The key facet-level parameters that effect the HETGS LRF are the grating period variations (both within and between facets) and the grating alignment, or "roll", variations (again within and between facets). The facet period, period variations, and roll variations were measured using the Laser Reflection setup[17].

In the Laser Reflection test a laser beam (HeNe 632.8 nm for MEGs and HeCd 325.0 nm for HEGs) is directed sequentially at an array of locations on each grating facet (10x11 or 11x12 locations). At each location the angle of the reflected and diffracted beams from the grating are measured and a local period is computed. The test setup includes MEG and HEG period references which are measured along with the sample and ensure the stability of the measurements. Each execution of the LR test creates an ASCII data file (13Kb or 16Kb) which can be analyzed to create a period contour map, Figure 4.1, and estimates of the grating average period, P, and period variations, "dp/p". The data can be re-analyzed limited to the "active" region that is expected to be illuminated by the HRMA to get a more accurate estimate of the grating's effect on performace.

The expected HETG equivalent dp/p is expected to be less than 130 ppm rms for both HEG and MEG gratings based on the data summarized in Figures 4.2-4.4.

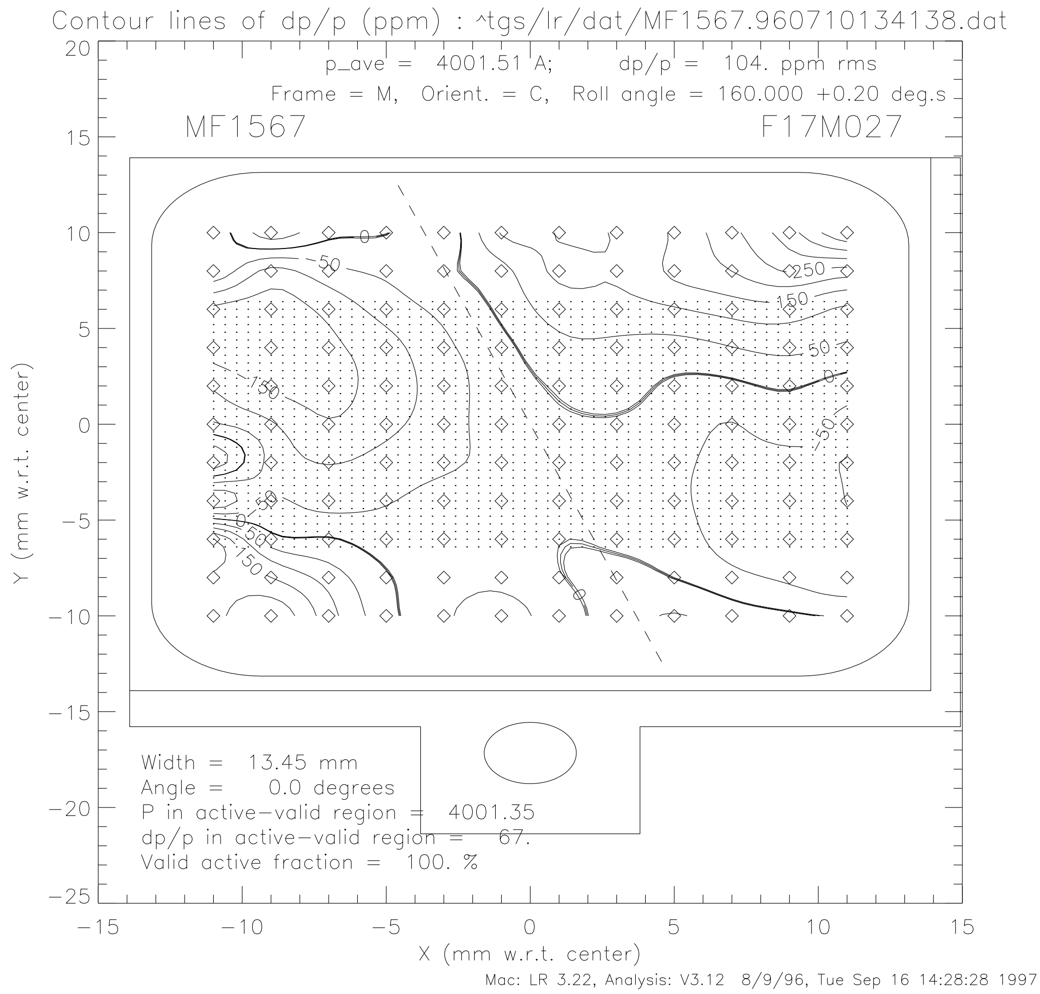

Figure 4.1: Period contour plot of MEG grating MF1567 from LR test data. Each diamond represents a measurement point. The dotted region is the "active" region that will be illuminated by X-rays from the HRMA. The period variation in the active region, dp/p = 67 ppm, is well below the required instrument variation of 250 ppm.

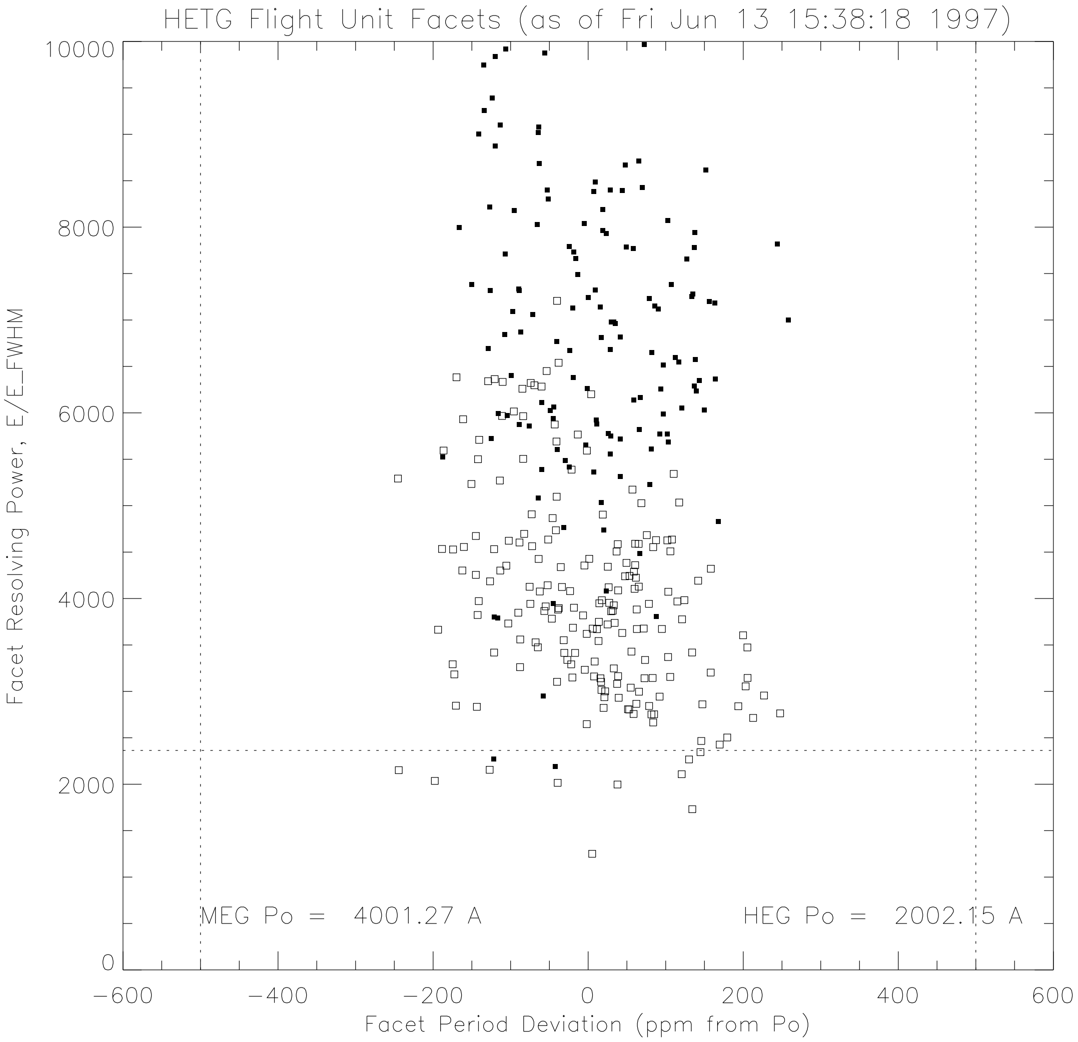

Figure 4.2: Period-dp/p scatter plot for the 336 HETG flight grating facets. The X-axis is each grating's departure from the average period for its type. The Y-axis is the inherent resolving power limit for the grating, that is: $(p/dp)(1/2.35)$. The horizontal dashed line at $E/dE \approx 2400$ corresponds to $dp/p = 180$ ppm.

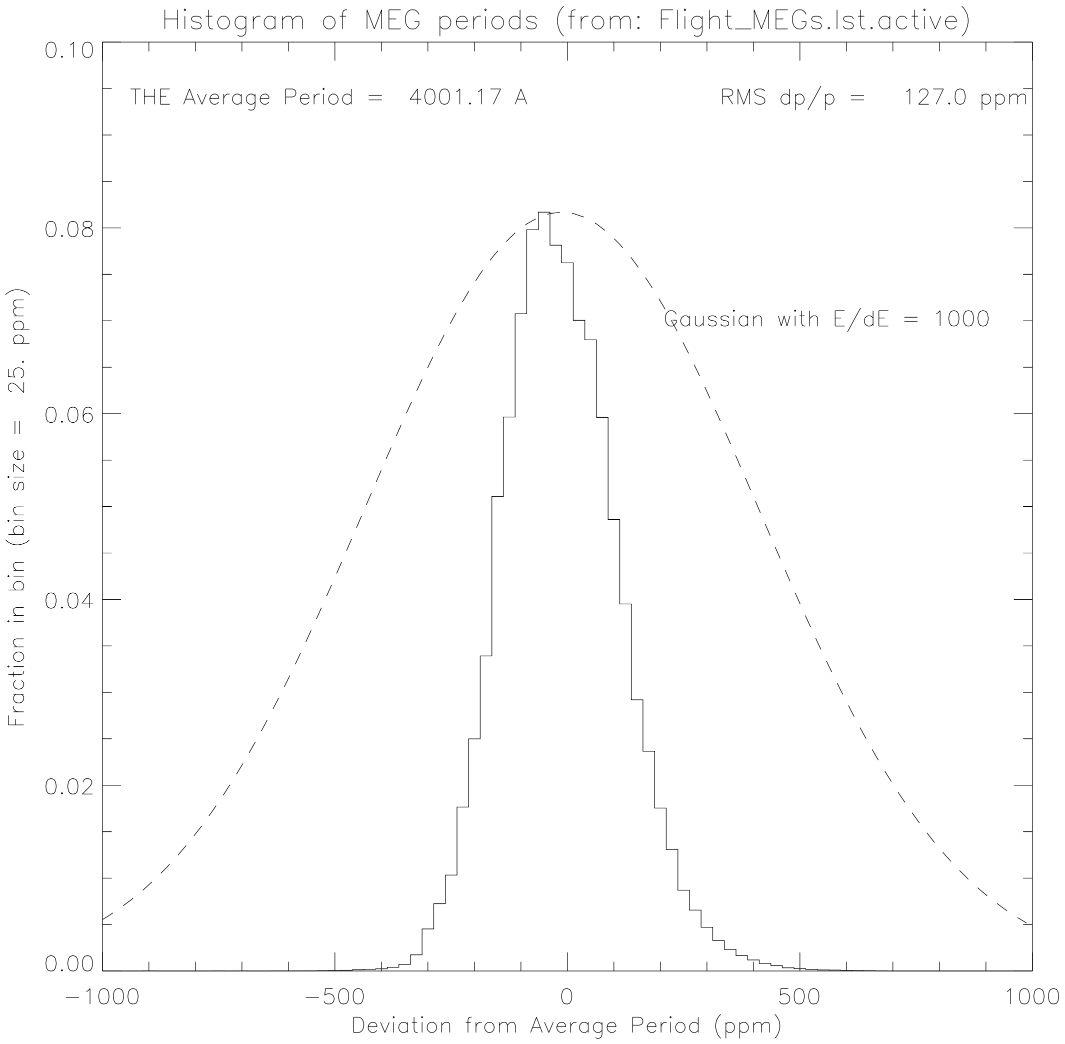

Figure 4.3: Period Histogram of the MEG Flight Gratings. The histogram and average period indicated here are based on the approximate "active" region of each facet. The rms dp/p value of 127 ppm corresponds to an E/dE limit of 3350. Note that the average period indicated here is in "LR-Å"; see Table 4.3 for the grating absolute periods.

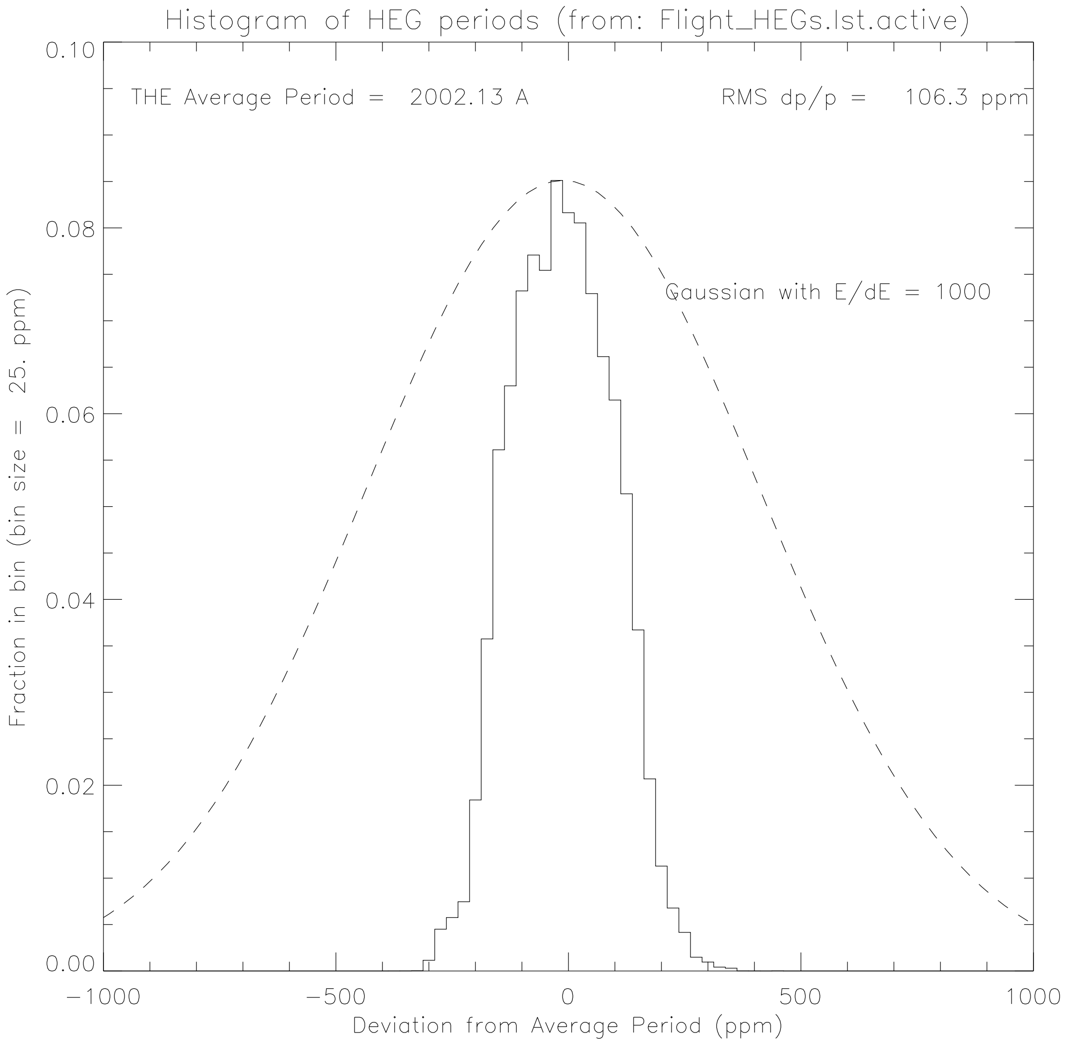

Figure 4.4: Period Histogram of the HEG Flight Gratings. The histogram and average period indicated here are based on the approximate "active" region of each facet. The rms dp/p value of 106.3 ppm corresponds to an E/dE limit of 4000. Note that the average period indicated here is in "LR-Å"; see Table 4.3 for the grating absolute periods.

4.1.2 LR Calibration using NIST Samples

The gratings on the flight HETG were each measured in the LR setup. The locations of the reflected and diffracted beams are measured from the grating under test and also from a fixed-in-the-instrument reference grating. Thus, all gratings are measured relative to fixed reference gratings (HEG or MEG). The periods of these reference gratings were assigned based on the laser wavelengths and the absolute diffraction angles (as measured by the encoded rotation stage.) The LR system has a high differential sensitivity and repeatability; however, its assigned periods are not expected to be absolutely accurate.

In order to set the absolute period of our reference gratings, we sent HEG and MEG calibration samples (on Silicon wafers) to John Kramar et al. at NIST (jkramar@NIST.GOV). They measured these HEG and MEG samples. Then these samples were measured by Dick Elder in the LR setup. From these measurements a *calibration factor* establishing the absolute period of our LR data is obtained, Table 4.2.

These calibration factors and errors are then applied to the measured average periods of the flight HETG and TOGA gratings yielding the final "LR-NIST" periods of Table 4.3.

Sample	NIST Period nm	NIST Error (1 σ) nm	LR Period Å[LR]	Calibration Factor Å/Å[LR]	Error ppm
NIST MEG	400.800	0.010	4007.74	1.00006	25.
NIST HEG	200.011	0.005	2001.43	0.999340	25.

Table 4.2: NIST samples for LR calibration

Grating	LR Average Period Å[LR]	LR-NIST Period Å	LR-NIST Error Å
Flight MEG	4001.17	4001.41	0.10
Flight HEG	2002.13	2000.81	0.05
TOGA MEG	4000.72	4000.96	0.10
TOGA HEG	2002.36	2001.04	0.05

Table 4.3: Correction of the LR Period Measurements

Please see http://space.mit.edu/HETG/sub_details.html

Figure 4.5: X-GEF Schematic

4.2 X-GEF Measurements

With the X-Ray Grating Evaluation Facility, X-GEF, at M.I.T. we have measured the diffraction efficiency of each flight grating at several energies and orders and fit these measurements to determine the physical-model parameters for each grating. From these best-fit parameters we can generate $g_f(E, m)$ for each grating on a fine energy scale.

The basic X-GEF test configuration is shown in Figure 4.5. The source of X-rays is an electron-impact source (Manson multi-anode) which has an X-ray spectrum that is made up of a continuum plus one or more discrete lines. The incoming X-ray beam, collimated by either a slit or 1-D optic, illuminates a grating. X-rays emerge from the grating into various diffraction orders and are detected by a position sensitive proportional counter, PSPC, which has a spatial range of +/- 60 mm. The goal of the measurement is to measure the fraction of the incoming beam (at the line energy) that is diffracted into the combined first-orders of the grating.

Because of the presence of continuum and other lines in the source and the poor energy resolution of the PSPC, there are many error sources that can foil a straight-forward measurement of the efficiency based only on with-grating/with-out-grating PSPC measurements. To avoid these pitfalls we have installed in X-GEF two gratings which serve as efficiency references, Section 3.2.5. During flight testing, measurements are also taken with the reference grating in the beam. The ratio of grating-under-test diffracted count rate to reference-grating diffracted count rate can then be made directly and with a much reduced sensitivity to systematic errors. In this way the known reference-grating efficiencies are transferred to the grating-under-test efficiencies.

Two gratings are tested in each unattended overnight X-GEF run. The $\approx$ 300 Mb of data collected are written to two DAT tapes (one stays at MIT and one goes to the ASC.) Figure 4.6 shows an example of the results of X-GEF data analysis[25] for an MEG grating. The measured plus and minus first order efficiencies at five energies (Cu L 0.930 keV, Mg K 1.254 keV, Al K 1.486 keV, Mo L 2.293 keV, and Ti K at 4.511 keV) are shown along with a model fit which uses a 5-vertex bar shape, Figure 4.8. For HEGs a measurement is additionally made at Fe K 6.400 keV, Figures 4.7 and 4.9.

These X-GEF model parameters and resulting model fits are the laboratory measure of $g_f(E, m)$ of Equation 1.4.

To-do:
Need a .ps version of the X-GEF schematic.
Add more details about the different regions tested.
Update X-GEF analysis and predictions when more accurate reference grating efficiencies are available.
Create table of measured asymmetry slopes for each grating-region to estimate HEG and MEG asymmetry slopes.

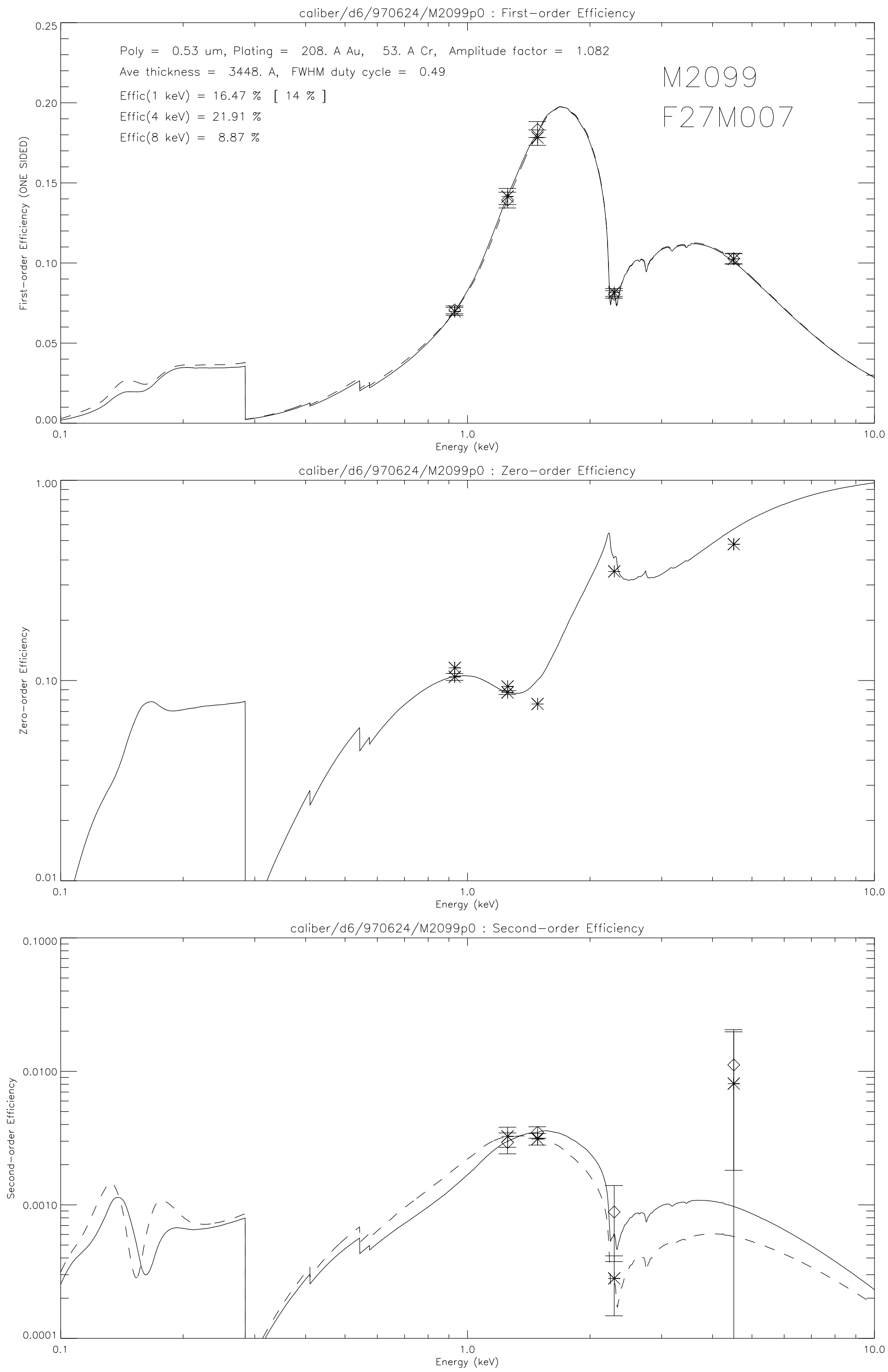

Figure 4.6: Measured and modeled first-order efficiency of the central region of MEG grating M2099. The model is simultaneously fit to +/- 1st-order, zero-order, and 2nd-order data. The interpolated combined efficiency at 1 keV of 16.47% exceeds the specification-required average of 14% .

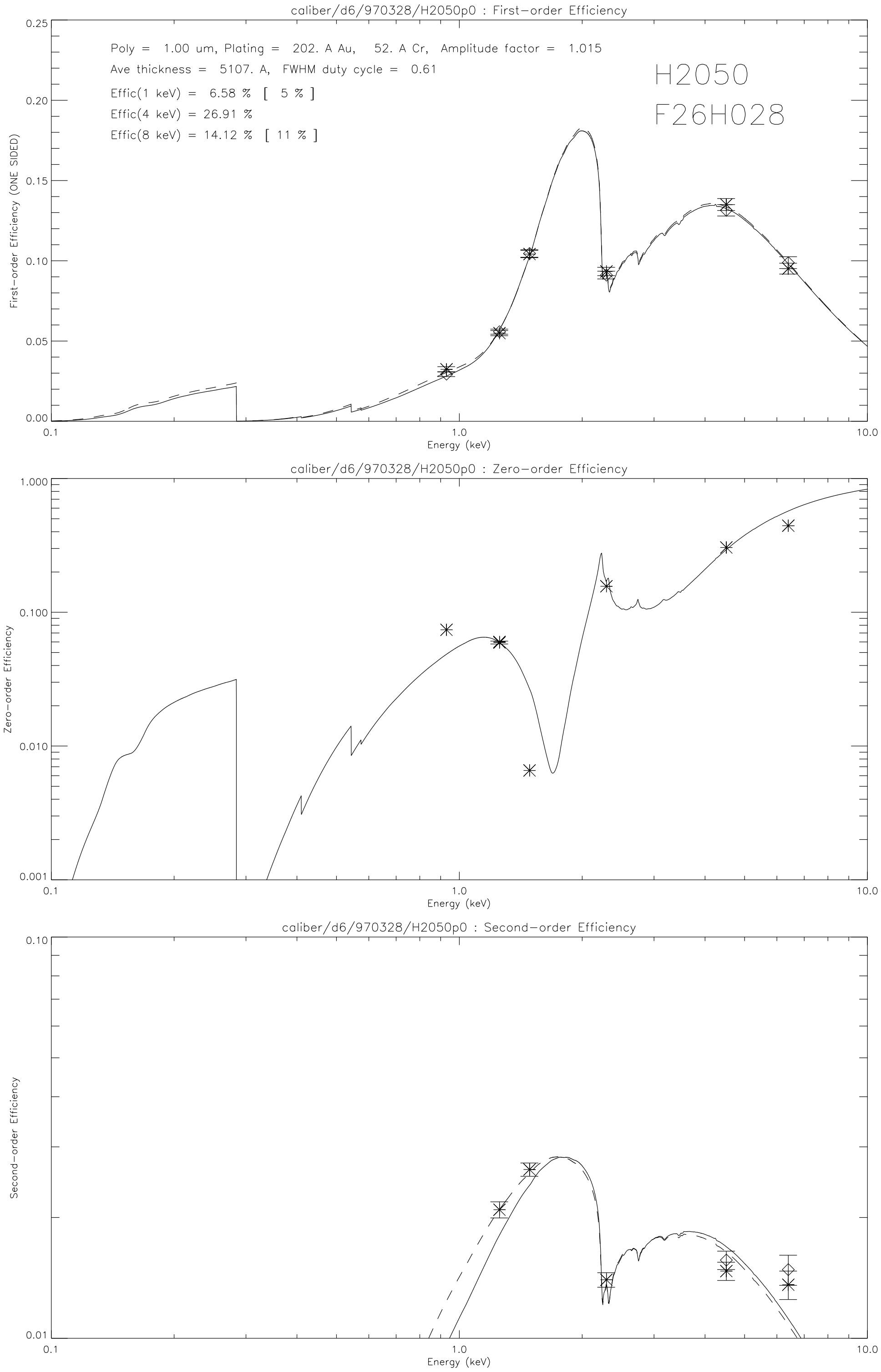

Figure 4.7: Measured and modeled first-order efficiency of the central region of HEG grating H2050. The model is simultaneously fit to +/- 1st-order, zero-order, and 2nd-order data. The interpolated combined efficiency at 8 keV of 14.1% exceeds the specification-required average of 11% .

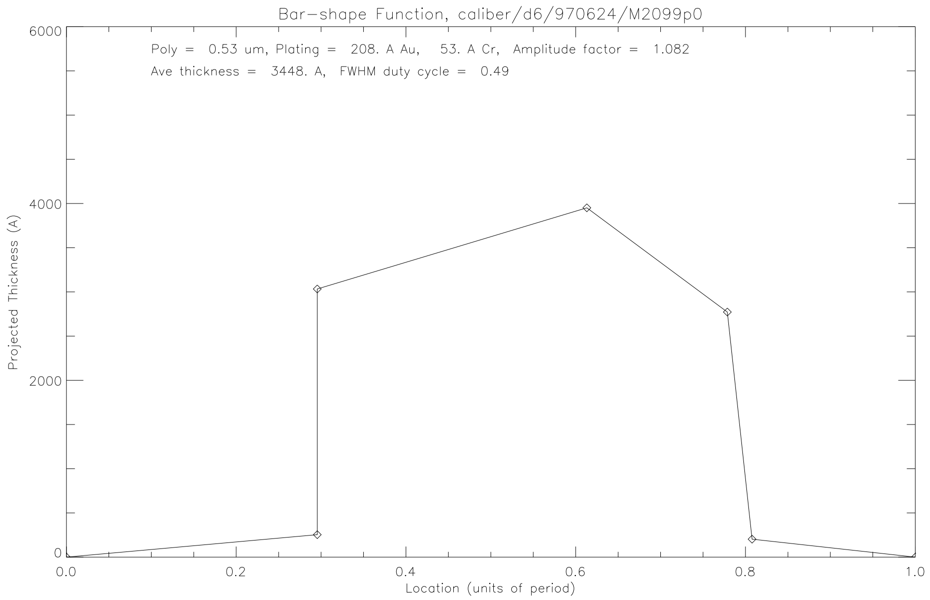

Figure 4.8: The 5-vertex bar shape used in the MEG model of Figure 4.6. The use of 5 adjustable vertices ensures a good fit of the model to the measured first-order efficiencies.

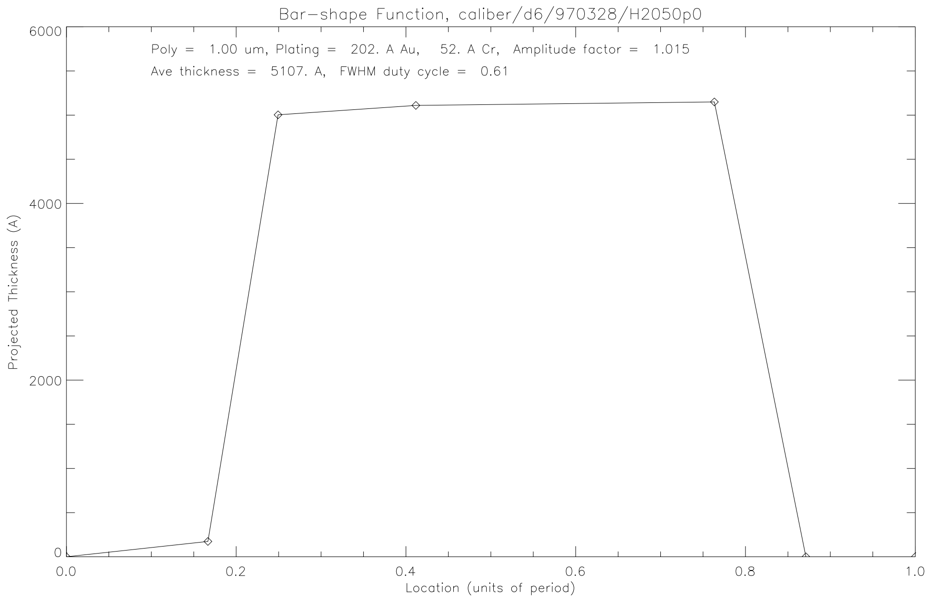

Figure 4.9: The vertex bar shape used in HEG the model of Figure 4.7. Note that the HEG shape here is thicker, wider, and more trapezoidal than the MEG example of Figure 4.8.

4.2.1 Order Assymmetry and Tilt

As expected by the diffraction theory, the trapezoidal profile of the gratings, when operated away from normal incidence, will produce an asymmetry in the intensity of the plus and minus diffracted orders. This asymmetry is measured routinely in X-GEF flight testing at the Al-K line, 1.486 keV. Figures 4.10 and 4.11 show the tilt test results for the example MEG and HEG gratings M2099 and H2050. Note the higher tilt sensitivity (steeper asymetry slope) of the HEG due to its more trapezoidal bar shape.

Because of the Rowland design of the HETG, the grating facets in use “see” X-rays arriving at normal incidence. For off-axis sources (due to multiple sources in the field or offset pointing of a desired source) the HETG may be called on to operate at angles of incidence of order 0.05 degrees (3 arc minutes or 9 mm off-axis.) Even for the HEG gratings this would result in an asymmetry of less than 2% between the plus and minus orders.

Note that the tilt curves are very linear within a degree of normal incidence (Grating Angle = 0). This means that the *total* first-order diffraction efficiency is very insensitive to small tilts. For this reason the primary efficiency calibration is the combined first-order values.

4.2.2 Laboratory Efficiency Predictions

The full set of model parameters derived from the X-GEF data are then used to create the shell-averaged efficiencies $G_s(E, m)$ for the full HETG. Coming into XRCF testing these represent out best estimate of expected HETG efficiency performance, Figures 7.13 and 7.14, and efficiency product, Section 9.3.4.

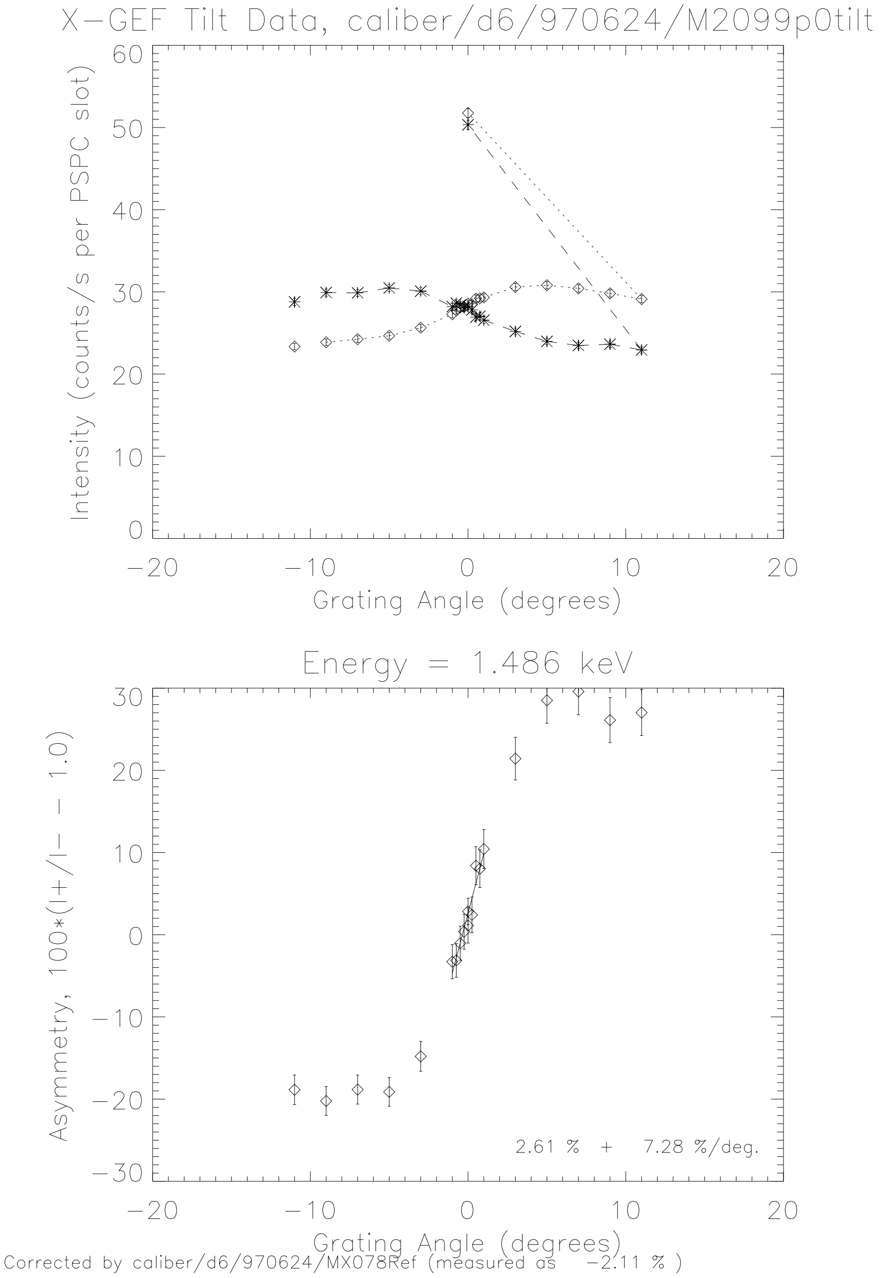

Figure 4.10: X-GEF Tilt Plots for an MEG. The top plot shows the plus and minus first-order Al-K count rates as a function of incidence angle. The bottom plot shows the "asymmetry" plotted versus angle. The normal-incidence asymmetry is only 2.6% with a slope of 7.3% per degree.

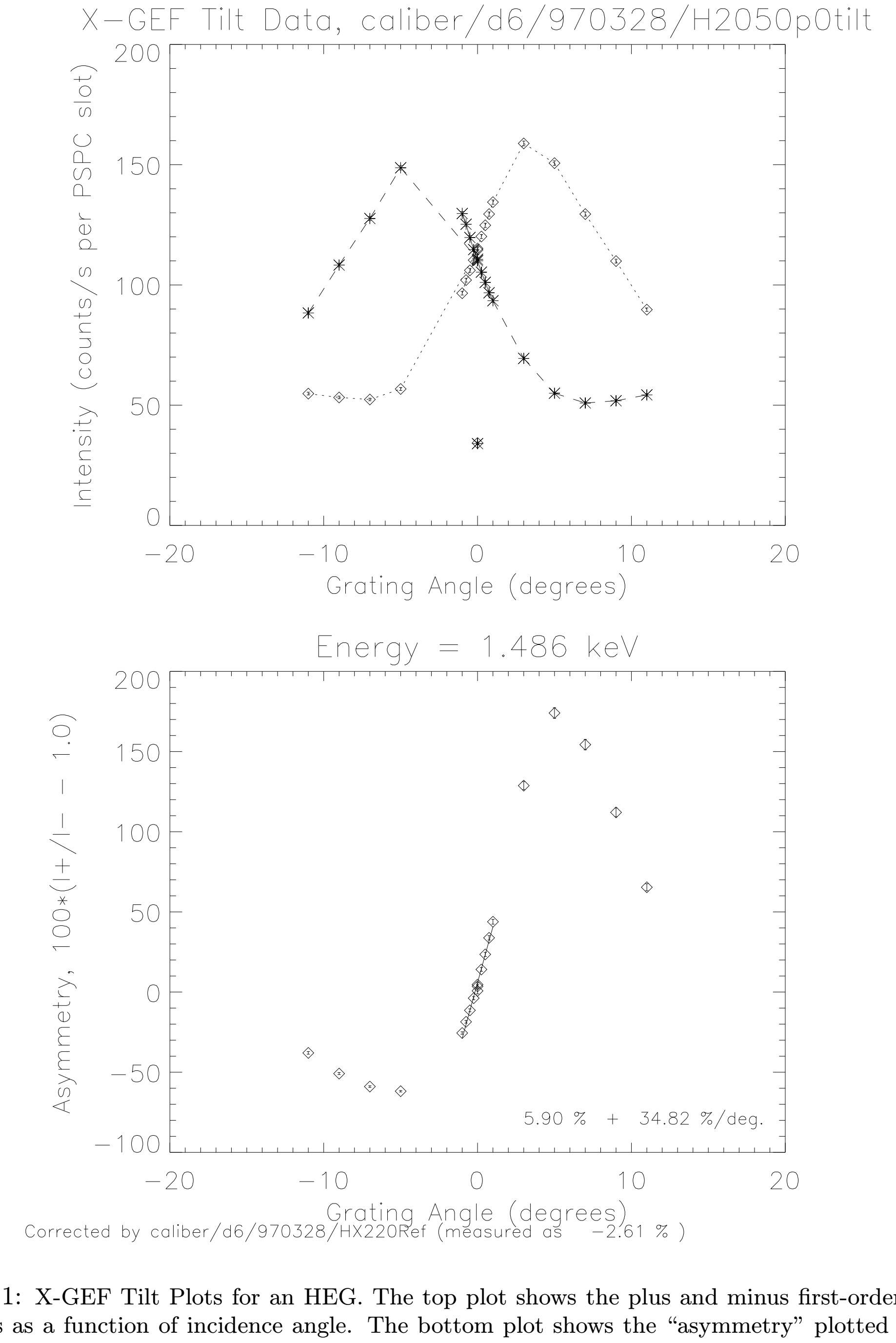

Figure 4.11: X-GEF Tilt Plots for an HEG. The top plot shows the plus and minus first-order Al-K count rates as a function of incidence angle. The bottom plot shows the "asymmetry" plotted versus angle. The normal-incidence asymmetry is 5.9% with a slope of almost 35% per degree. This strong asymmetry with angle is the result of the trapezoidal shape of the grating bar, Figure 4.9.

4.3 Alignment Measurements

The facet-to-facet alignment variations were measured as part of the facet installation procedure; the roll angle of each facet with respect to a reference facet was measured in the HETG Alignment Facility based on the polarization alignment technique of Anderson *et al.*[4]. The total roll variation of the facets is measured with the polarization technique to be well below our design specification of 1.1 arc minutes rms, Figure 4.12.

To-do: Describe the measurements regarding polyimide effects on the polarization-measured angle.

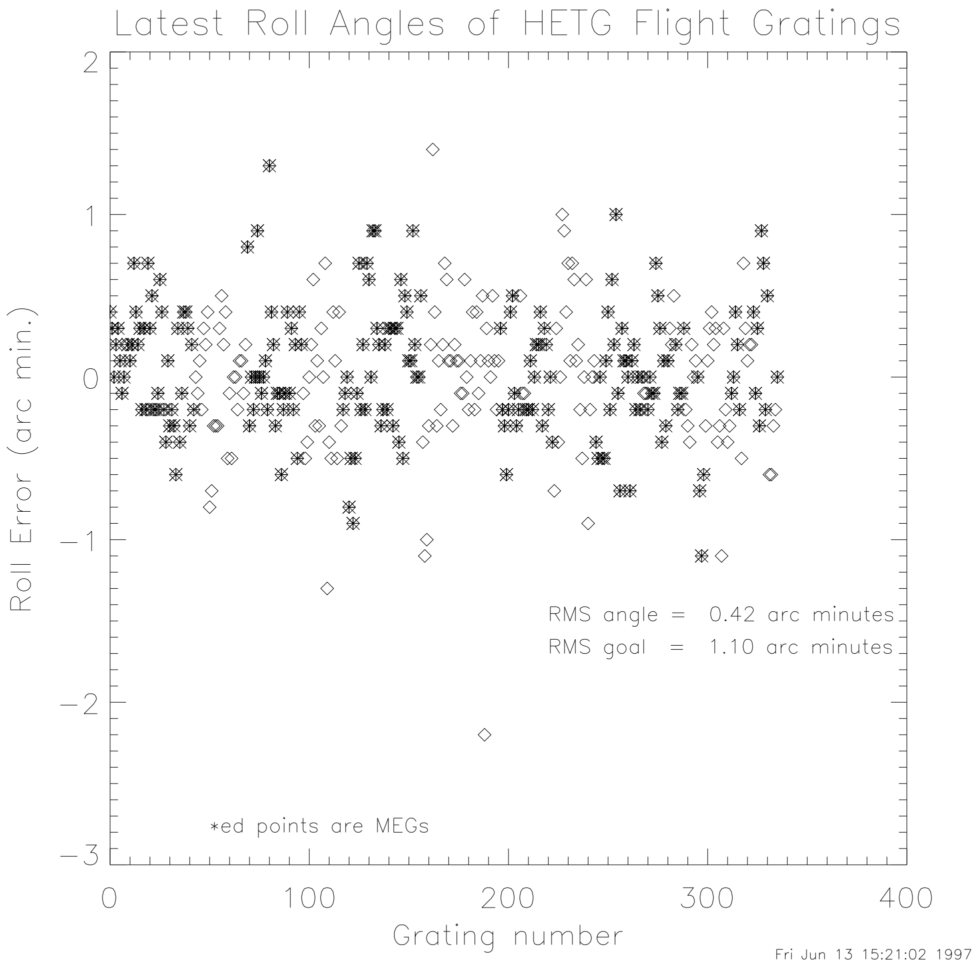

Figure 4.12: Measured roll errors for the 336 flight gratings. The rms value $\gamma = 0.42$ arc minutes is well below the specification of 1.1 arc minutes.

4.4 Long-term: Vacuum Storage Gratings

A sample of HETG gratings has been aged in a high vacuum environment and measured in the LR and X-GEF setups periodically since late 1996 to determine if there are any changes ("aging") in the performance parameters. The evaluations in early 1998 indicate that there are no trends that would change the calibration of the HETG instrument. Several changes in performance parameters have been detected but most seem to be caused by measurement or sample anomolies. Aging and evaluation of these gratings will continue and updates will be made as testing is completed. For more information see `http://space.mit.edu/HETG/vsg/vsg.html`.

4.5 Optical Transmission of the Gratings

Gratings MA1046, HA2044, HA2031, and M2214 were provided to Prof. Gordon Garmire of PSU for optical transmission measurements.

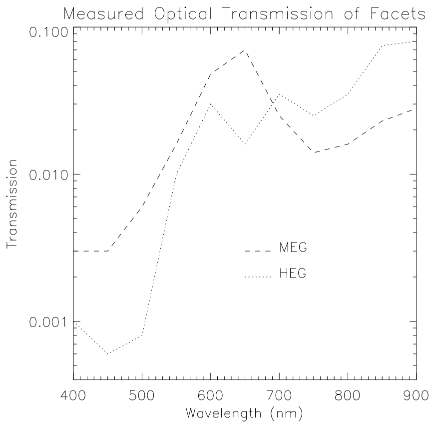

Figure 4.13: Measure transmission of two grating facets in the optical range. Data taken from Garmire *et al.*[29].